

Analysis of the tsunami generated by the M_w 7.8 1906 San Francisco earthquake

Eric L. Geist
Mary Lou Zoback

U.S. Geological Survey, 345 Middlefield Road, Menlo Park, California 94025, USA

ABSTRACT

We examine possible sources of a small tsunami produced by the 1906 San Francisco earthquake, recorded at a single tide gauge station situated at the opening to San Francisco Bay. Coseismic vertical displacement fields were calculated using elastic dislocation theory for geotectonically constrained horizontal slip along a variety of offshore fault geometries. Propagation of the ensuing tsunami was calculated using a shallow-water hydrodynamic model that takes into account the effects of bottom friction. The observed amplitude and negative pulse of the first arrival are shown to be inconsistent with small vertical displacements (~4–6 cm) arising from pure horizontal slip along a continuous right bend in the San Andreas fault offshore. The primary source region of the tsunami was most likely a recently recognized 3 km right step in the San Andreas fault that is also the probable epicentral region for the 1906 earthquake. Tsunami models that include the 3 km right step with pure horizontal slip match the arrival time of the tsunami, but underestimate the amplitude of the negative first-arrival pulse. Both the amplitude and time of the first arrival are adequately matched by using a rupture geometry similar to that defined for the 1995 M_w (moment magnitude) 6.9 Kobe earthquake: i.e., fault segments dipping toward each other within the stepover region (83° dip, intersecting at 10 km depth) and a small component of slip in the dip direction (rake = -172°). Analysis of the tsunami provides confirming evidence that the 1906 San Francisco earthquake initiated at a right step in a right-lateral fault and propagated bilaterally, suggesting a rupture initiation mechanism similar to that for the 1995 Kobe earthquake.

INTRODUCTION

Teleseismic recordings, stopping of astronomical clocks, and a single strong ground motion record all indicate an epicentral location for the M_w (moment magnitude) 7.8 1906 San Francisco earthquake on the San Andreas fault in the region just offshore from San Francisco (Bolt, 1968; Boore, 1977). In this study, we show that the epicentral region was also the source region for a small, 10 cm tsunami generated by the 1906 earthquake and recorded at a San Francisco tide gauge station. Because of the importance of the 1906 earthquake on earthquake hazard assessments in the San Francisco Bay area, there have been several recent studies to better define the source parameters for this event (Wald et al., 1993; Thatcher et al., 1997; Zoback et al., 1999). Thatcher et al. (1997) resolved the horizontal fault slip along the 1906 rupture from triangulation data, including several local geodetic networks. Two of the local nets, Tomales Bay and Colma, provide reasonably well constrained endpoint estimates of horizontal slip, ranging from 3.6 to 4.5 m, bracketing the portion of the fault offshore of the Golden Gate (Thatcher et al., 1997). We use this geotectonically constrained slip estimate and the tsunami record to infer the probable rupture geometry along this offshore segment of the San Andreas fault.

The tsunami was recorded at the only northern California tide gauge station operating at the

time, located in San Francisco. The tsunami was first described in Lawson (1908) as a lowering of sea level of ~10 cm for a duration of ~16 min soon after the earthquake. In a recent study of the tsunami, Ma et al. (1991) inverted the observed waveform to determine the coseismic vertical component of sea-floor motion over a 300 km² horizontal grid. At the time of that study, little was known about the geometry of faulting offshore, and the authors were unable to ascribe the sea-floor deformation to slip along individual fault strands, though they did recognize the role the right-stepping bend in the fault must have had on generation of the tsunami. Recent analysis of the offshore fault structure in the 1906 epicentral region by Zoback et al. (1999) summarized here, however, provides more detailed information to test whether or not rupture occurred on discontinuous strands of the fault offshore.

NEW OFFSHORE FAULT INTERPRETATION

In the southern San Francisco Peninsula, the San Andreas fault makes a broad (~10°–11°) left (restraining) bend, following the crest of the late Pliocene-Quaternary Coast Ranges (e.g., Burgmann et al., 1994). Less than 70 km to the northwest, the San Andreas fault trace is below sea level. Projection of the onshore traces northwest of Lake Merced and southeast of Bolinas Lagoon suggests a 2–3 km right step or bend offshore on

the Golden Gate platform (Fig. 1). Linear, pseudo-gravity maximum gradients inferred from the shortest wavelengths of a new high-resolution aeromagnetic survey reveal in detail the right-stepping geometry for both the San Andreas and subparallel San Gregorio fault zones on the Golden Gate platform (Jachens and Zoback, 1998; Zoback et al., 1999).

In this study an ~3 km right step is assumed in the San Andreas fault just offshore from Lake Merced (following Zoback et al., 1999) (Fig. 1). The location and position of the inferred right step are consistent with interpretation of single-channel, high-resolution seismic reflection profiles (Fig. 1, identified by Cooper, 1973, as the “recent trace of the San Andreas fault”). The newly defined easternmost strand of the San Andreas fault extends northwest to the east side of Bolinas Lagoon, whereas the 1906 rupture lies along the west side of Bolinas Lagoon, implying an additional small (~1 km) left step offshore. Cooper also identified such a left step in his interpretation of the San Andreas fault just north of lat. 37°51′ (Fig. 1). North of this point, the San Andreas fault trace mapped by him coincides with the fault segment inferred from aeromagnetic analysis that connects with the 1906 surface trace on the west side of Bolinas Lagoon. Thus, the available offshore data suggest an ~3 km extensional right step and a smaller (~1 km) compressional left step in the San Andreas fault on

the Golden Gate platform. Bolt's (1968) teleseismic location for the 1906 earthquake is close to the right stepover (Fig. 1). Zoback et al. (1999) have suggested that the bilateral 1906 rupture may have nucleated in the right stepover region of the San Andreas fault, on the basis of similarities to the 1995 Kobe earthquake bilateral rupture, which also initiated in a similar right step in a right-lateral fault (Wald, 1996). Segall and Pollard (1980) demonstrate that normal traction along a right-lateral fault decreases at a right-stepping discontinuity, facilitating sliding.

TSUNAMI RECORD AND MODELING

The tsunami generated by the 1906 earthquake was recorded at the Presidio tide gauge station ~2 km east of the present-day tide gauge station located at Fort Point beneath the southern end of the Golden Gate bridge (Fig. 1). The tidal signal was removed from the digitized tide gauge record by calculating tidal harmonic constants for the observation site (Foreman, 1993). The record indicates that the primary tsunami signal was a lowering of sea level about 10 cm over about 16 min (Fig. 2; inset shows original tide gauge record from Lawson, 1908). Ambient short-period wave energy due to meteorological effects is apparent in the tide-gauge record for two days preceding the earthquake, slowly diminishing but continuing through the time the tsunami was recorded (Disney and Overshiner, 1925). Absolute timing on the original record is not precise nor is the exact origin time of the earthquake known. However, the onset of an interval of strong shaking (noted as "blurred by earthquake" on the original record) probably represents the direct P- and S-wave arrivals. For a 10-km-deep hypocenter (consistent with the geodetic slip model) located 8–10 km from the tide gauge station, the direct P-wave traveltime would be ~3 s with a direct S-wave arriving about 2 s later (assuming average P- and S-wave velocities of 5.7 and 3.3 km/s, respectively; Holbrook et al., 1996). The initial lowering of the main tsunami pulse started about 7 min later. Several sea-level fluctuations with apparent periods of 40–45 min. are apparent in the record following the initial negative pulse (which Lawson, 1908, reported was unique in eight years of records from this station). Lawson (1908) attributed these later arrivals to waves trapped and reflected within San Francisco Bay.

Tsunamis are gravity waves generated by the vertical movement of the sea floor during an earthquake. Tsunami propagation depends on the local bathymetry, and because the wavelength of a tsunami is often many times greater than the water depth, propagation is modeled using shallow-water wave theory. To forward model the tsunami generated by the 1906 San Francisco earthquake, we first computed the vertical component of sea-floor displacement using elastic dislocation theory (Okada, 1992) for a variety of

offshore rupture geometries. For this application, we ignore inelastic deformation, localized changes in slip magnitude, and possible secondary fracturing that may occur during rupture (Segall and Pollard, 1980). To compute the tsunami, we modified a hydrodynamic model developed by Casulli (1990) and Cheng et al. (1993) to study tidal circulation in San Francisco Bay. The model is based on a semi-implicit, finite-difference form of the nonlinear, shallow-water wave equations, and includes the effects of bottom friction. This model is unconditionally stable and is not required to satisfy stability criteria traditionally used in tsunami models. The model is modified by replacing the tidal-forcing boundary conditions with passive, radiation boundary conditions and adding an initial condition represented by vertical sea-floor displacement. During propagation, the tsunami is assumed to be perfectly reflected along all of the shorelines. The model domain is expanded from the San Francisco Bay estuarine study of Cheng et al. (1993) to include the offshore region of the Golden Gate platform, extending ~30 km to the north and south of the Golden Gate, using bathymetry calculated from soundings made during several U.S. Geological Survey cruises in the region. Tsunami calculations were performed on a 250 m grid at a time interval of 35 s.

OFFSHORE RUPTURE SCENARIOS

The principal objective of modeling the tsunami from the 1906 earthquake is to attempt to constrain some of the details of the offshore rupture, for example, to determine whether rupture occurred on a continuous offshore strand of the San Andreas fault or whether rupture occurred on discontinuous strands with a possible component of dip slip. In each case, the horizontal component of slip in the offshore region is interpolated from estimates provided by local geodetic networks to the north and south of the Golden Gate platform (Thatcher et al., 1997). Three possible rupture scenarios were examined; a map of sea-floor subsidence together with the observed and predicted tide gauge record at the Presidio station are shown in Figure 3.

Scenario A represents a continuous offshore rupture with a small right bend, along the fault trend of Thatcher et al. (1997). All fault segments are assumed to be vertical, and slip is purely horizontal. Dislocation modeling predicts a maximum subsidence of 4–5 cm in the vicinity of the right bend, directly across from the Golden Gate (Fig. 3A). Comparison of the synthetic with the observed record indicates a poor fit: The negative amplitude arrival is significantly smaller and earlier than observed. Rupture scenario B for the 1906 earthquake (Fig. 3B) includes the right stepover and a local change of dip in the stepover region to 83°, such that the two fault strands intersect at an assumed focal depth of 10 km. Owing to the inclusion of the stepover, the syn-

thetic record produced by horizontal slip on discontinuous fault strands better matches the arrival time of the tsunami on the observed record; however, the amplitude of the primary negative arrival is slightly less than what was recorded. The largest coseismic vertical displacements (~6–7 cm) are localized in the region of the right step. Overall, the comparison between the synthetic and observed records for this case is good and strongly suggests that the 1906 rupture occurred on the discontinuous fault strands defined by aeromagnetic anomalies (Fig. 1).

The third rupture scenario considered is analogous to rupture of the 1995 M_w 6.9 Kobe earthquake. The source process of this earthquake has been well determined in previous studies (e.g., Wald, 1996; Spudich et al., 1998) and indicates that, like the 1906 San Francisco earthquake, the epicenter for the 1995 Kobe earthquake is located in a right stepover region. Furthermore, these studies also indicate that the rake of the slip vectors in the Kobe stepover region deviate from horizontal and that fault segments in this region dip toward each other, intersecting near the hypocentral depth. Scenario C is similar to scenario B but with a local change in rake to -172° , similar to what was observed for the Kobe earthquake (equivalent to 0.5 m dip-slip motion in addition to the ~4 m of strike-slip motion). Both of these factors increase the local vertical displacement in the right stepover region: The average subsidence in this region (covering ~12.5 km²) is ~50 cm, and maximum subsidence is about 70 cm. In addition, a small (~1 km) left stepover south of Bolinas Lagoon is included in this scenario. Largely because of the small component of dip slip in the right stepover, the amplitude and first arrival time of the tsunami derived from this rupture scenario closely match the observed amplitude (Fig. 3C) as well as some of the waveform complexity observed in the early part of the record. The predicted trailing positive peak, however, is not observed in the record.

To investigate the possibility that the elastic limit was exceeded in the stepover region we also ran each of the scenarios using a Poisson's ratio of 0.45 to more closely preserve volume. The higher Poisson's ratio tended to concentrate the deformation near the fault and increase tsunami amplitudes. There was little change in the predictions for scenario A, supporting the conclusion that the marigram indicates localized deformation associated with a stepover, rather than a simple fault bend. The increased amplitudes for the higher Poisson's ratio for scenario B improved the fit to the marigram, although initial complexity of the marigram was better fit with Scenario C.

Another possible tsunami source considered in this study is massive cliff failures that occurred during the 1906 earthquake where the San Andreas fault intersects the coastline ~15 km south of Fort Point (Lawson, 1908). Despite the

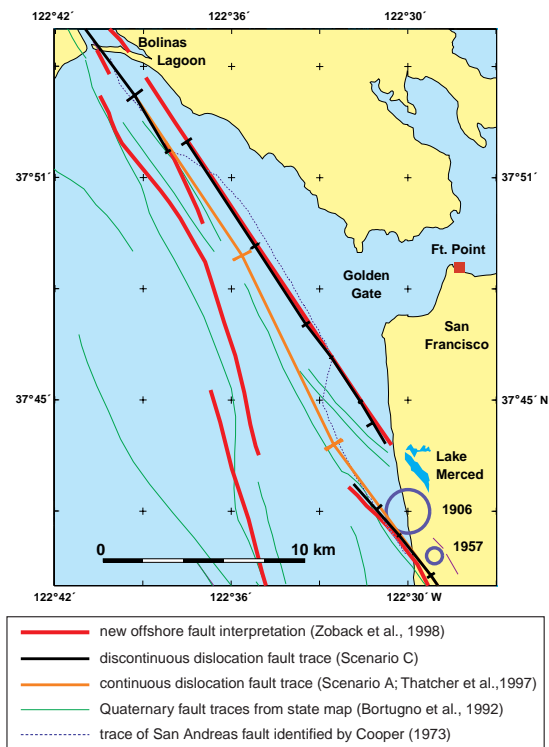


Figure 1. Possible fault geometries on Golden Gate platform. Inferred offshore fault structure is determined from gradient analysis of new high-resolution aeromagnetic data (Jachens and Zoback, 1998; Zoback et al., 1999) given by heavy red lines. Hachures indicate boundaries of individual fault segments used in dislocation modeling. Blue circles indicate epicenters of 1906 M_w 7.8 (Bolt, 1968) and 1957 M 5.3 probable normal faulting earthquake (Marsden et al., 1995).

Figure 3. Sea-floor subsidence from dislocation modeling and comparison of synthetic and observed records. Scenario A: Pure horizontal slip on continuous vertical strike-slip fault with right bend offshore (after Thatcher et al., 1997). Scenario B: Pure horizontal slip on discontinuous fault segments separated by 3 km right step near Lake Merced. Slip vectors in this region have rake of -172° . Scenario C: Discontinuous rupture separated by 3 km right step as in B and 1 km left step near Bolinas Lagoon. Fault segments in right step dip inward at 83° .

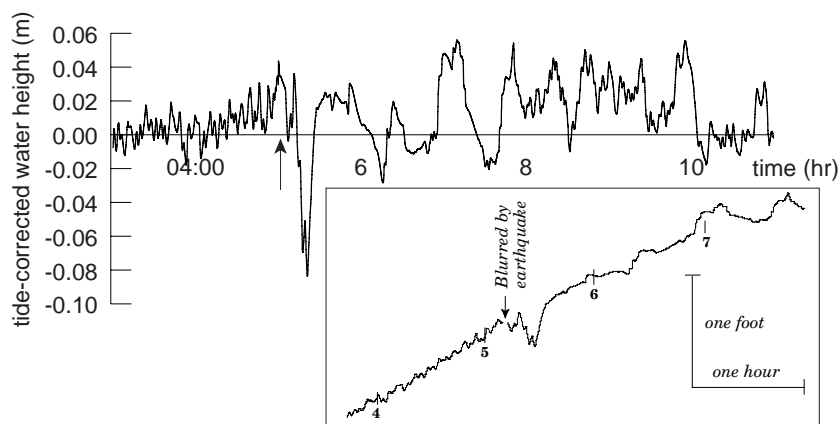
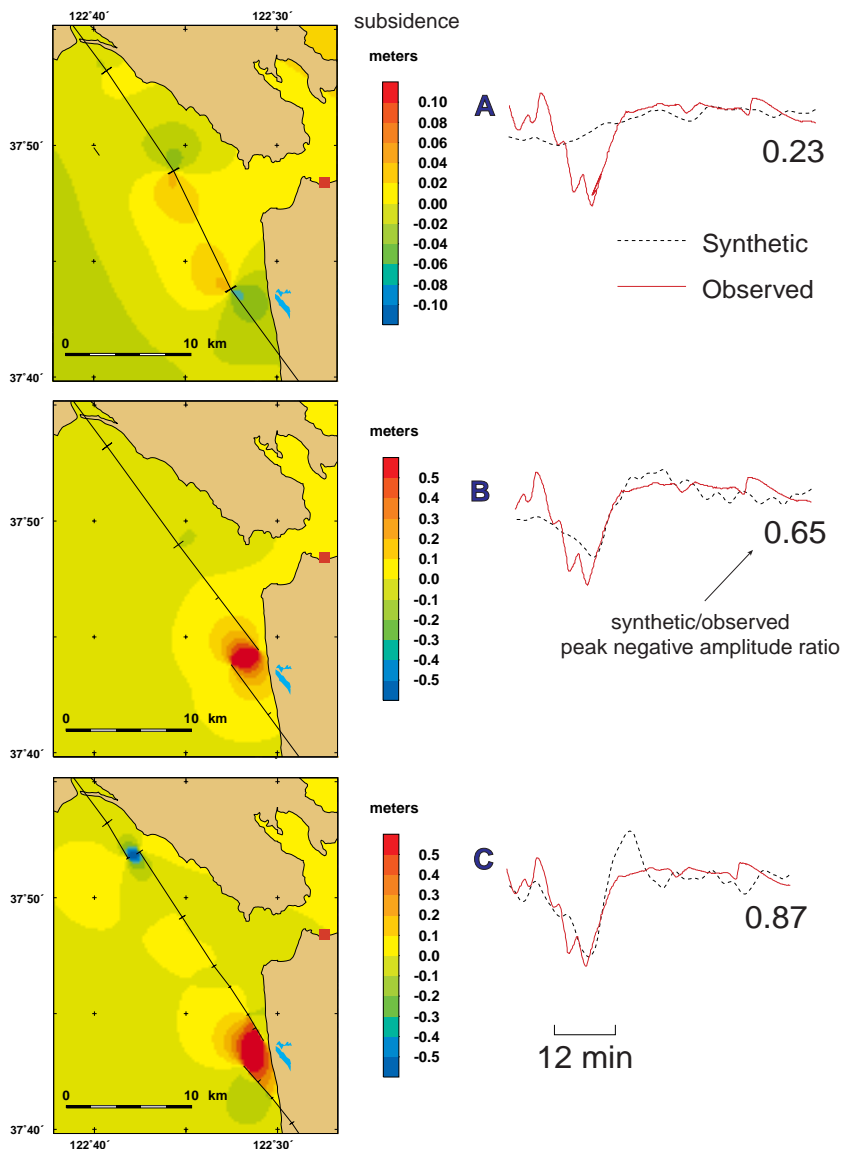


Figure 2. Tide gauge record on April 18, 1906, from Presidio tide gauge station with tidal signal removed. Arrow indicates approximate origin time of earthquake. Inset shows original record from Lawson (1908).



difficulty in establishing accurate initial conditions for a tsunami caused by cliff failure, predicted traveltimes alone indicates that a cliff-failure tsunami in this location would arrive too late to explain the observed record.

Using the rupture scenario for the 1906 San Francisco earthquake analogous to the 1995 Kobe earthquake (scenario C), examination of the full tsunami time history reveals several interesting hydrodynamic phenomena. First, coastal trapped waves propagating parallel to the coastline are apparent, similar to the tsunami generated from the 1992 M_w 7.2 Cape Mendocino earthquake (González et al., 1995). The trapped waves are eventually reflected back toward the Golden Gate by the irregular coastline, providing an alternate explanation for the later arrivals observed in the tsunami record rather than the explanation proposed initially by Lawson (1908) as reverberation within San Francisco Bay. The hydrodynamic modeling indicates that the tsunami is significantly attenuated as it passes through the Golden Gate and attenuated further as it propagates to the north and south in the shallow reaches of San Francisco Bay. Little, if any, tsunami energy within San Francisco Bay is reflected back through the Golden Gate.

CONCLUSIONS

Hydrodynamic modeling of the tsunami generated by the 1906 San Francisco earthquake and recorded at the Presidio tide gauge station suggests that rupture occurred on discontinuous strands of the San Andreas fault at a right stepover south of the Golden Gate, the location of which is constrained by the arrival time of the tsunami. The tsunami is not consistent with subsidence accompanying the pure horizontal slip on a continuous rupture in the offshore region or by massive cliff failures reported where the San Andreas fault intersects the coast line 15 km south of the Golden Gate. Changes in the fault dip and rake in the epicentral stepover region (83° inward and -172° , respectively) analogous to the 1995 Kobe earthquake produce a record very similar to that observed, but this scenario (C) cannot be unequivocally distinguished from the horizontal rake scenario (B) using the single existing record of the tsunami. Like the tsunami accompanying the 1992 Cape Mendocino earthquake, the tsunami caused by the 1906 San Francisco may have generated energetic, coastal-trapped waves. In contrast, our models suggest that the tsunami appears to have been greatly attenuated as it entered San Francisco Bay. That the epicenters for both the 1906 San Francisco and 1995 Kobe earthquakes were located in a right stepover of a right-lateral fault suggests similar rupture initiation mechanisms (Zoback et al., 1999).

ACKNOWLEDGMENTS

Reviews by R. W. Simpson, K. Satake, A. S. Meltzer, and T. E. Parsons greatly improved the manuscript. Dislocation modeling was performed using code developed by R. W. Simpson based upon Okada's (1992) elastic dislocation theory. We thank R. W. Simpson, R. T. Cheng, and J. W. Gartner for patiently answering our many questions about their codes. Special thanks to Chris Stevens for digitizing the original tsunamis record from Lawson (1908).

REFERENCES CITED

- Bolt, B. A., 1968, The focus of the 1906 California earthquake: *Seismological Society of America Bulletin*, v. 58, p. 457–471.
- Boore, D. M., 1977, Strong-motion recordings of the California earthquake of April 18, 1906: *Seismological Society of America Bulletin*, v. 67, p. 561–577.
- Bortugno, E. J., McJunkin, R. D., and Wagner, D. L., 1992, Map showing recency of faulting, San Francisco–San Jose quadrangle, California: California Division of Mines and Geology Regional Geologic Map Series, Map 51, sheet 5, scale 1:250,000.
- Burgmann, R., Arrowsmith, R., Dumitru, T., and McLaughlin, R., 1994, Rise and fall of the southern Santa Cruz Mountains, California, from fission tracks, geomorphology, and geodesy: *Journal of Geophysical Research*, v. 99, p. 20181–20202.
- Casulli, V., 1990, Semi-implicit finite difference methods for the two-dimensional shallow water equations: *Journal of Computational Physics*, v. 86, p. 56–74.
- Cheng, R. T., Casulli, V., and Gartner, J. W., 1993, Tidal, residual, intertidal mudflat (TRIM) model and its applications to San Francisco Bay, California: *Estuarine, Coastal and Shelf Science*, v. 35, p. 235–280.
- Cooper, A. K., 1973, Structure of the continental shelf west of San Francisco, California: U.S. Geological Survey Open-File Report 73-1907, 65 p.
- Disney, L. P., and Overshiner, W. H., 1925, Tides and currents in San Francisco Bay: U.S. Coast and Geodetic Survey Special Publication, 115, 125 p.
- Foreman, M. G. G., 1993, Manual for tidal height analysis and prediction (revised): Sidney, British Columbia, Institute of Ocean Sciences, Pacific Marine Science Report 77-10, 66 p.
- González, F. I., Satake, K., Boss, E. F., and Mofjeld, H. O., 1995, Edge waves and non-trapped modes of the 25 April 1992 Cape Mendocino tsunami: *Pure and Applied Geophysics*, v. 144, p. 409–426.
- Holbrook, W. S., Brocher, T. M., ten Brink, U. S., and Hole, J. A., 1996, Crustal structure of a transform plate boundary: San Francisco Bay and the central California continental margin: *Journal of Geophysical Research*, v. 101, p. 22311–22334.
- Jachens, R. C., and Zoback, M. L., 1998, The San Andreas fault in the San Francisco Bay region, California: Structure and kinematics of a young plate boundary: *International Geology Review*, (in press).
- Lawson, A. C., 1908, The California earthquake of April 18, 1906, Report of the State Earthquake Investigation Commission (volumes I and II): Washington, D.C., Carnegie Institute.
- Ma, K. F., Satake, K., and Kanamori, H., 1991, The origin of the tsunami excited by the 1906 San Francisco earthquake: *Seismological Society of America Bulletin*, v. 81, p. 1396–1397.
- Marsden, R., Zoback, M. L., Dreger, D., Julian, B., Olson, J., and Parsons, T., 1995, M5.3 normal? faulting event adjacent to the San Andreas fault on the San Francisco Peninsula: *Eos (Transactions, American Geophysical Union)*, v. 76, p. F423.
- Okada, Y., 1992, Internal deformation due to shear and tensile faults in a half-space: *Seismological Society of America Bulletin*, v. 82, p. 1018–1040.
- Segall, P., and Pollard, D. D., 1980, Mechanics of discontinuous faults: *Journal of Geophysical Research*, v. 85, p. 4337–4350.
- Spudich, P., Guatteri, M., Otsuki, K., and Minagawa, J., 1998, Use of fault striations and dislocation models to infer tectonic shear stress during the 1995 Hyogo-ken Nanbu (Kobe) earthquake: *Seismological Society of America Bulletin*, v. 88, p. 413–427.
- Thatcher, W., Marshall, G., and Lisowski, M., 1997, Resolution of fault slip along the 470-km-long rupture of the great 1906 San Francisco earthquake and its implications: *Journal of Geophysical Research*, v. 102, p. 5353–5367.
- Wald, D. J., 1996, Slip history of the 1995 Kobe, Japan, earthquake determined from strong-motion, teleseismic, and geodetic data: *Journal of Physics of the Earth*, v. 44, p. 489–503.
- Wald, D. J., Kanamori, H., Helmberger, D. V., and Heaton, T. H., 1993, Source study of the 1906 San Francisco earthquake: *Seismological Society of America Bulletin*, v. 83, p. 981–1019.
- Zoback, M. L., Jachens, R. C., and Olson, J. A., 1999, Abrupt along-strike change in tectonic style: San Andreas fault zone, San Francisco peninsula: *Journal of Geophysical Research* (in press).

Manuscript received May 26, 1998

Revised manuscript received September 22, 1998

Manuscript accepted October 6, 1998